#3538

Combining Door Swing Pumping with Density Driven Flow

D.E. Kiel D.J. Wilson

ABSTRACT

Measurements of exchange flows through doorways were made in a test house and in a geometrically similar 1:20 scale model. A tracer gas was used in the full-scale study to determine the volume of air exchanged during opening-closing cycles over a range of temperature differences from 0°C to 34°C across the doorway. The 1:20 model simulation utilized salt water and fresh water to simulate the density difference caused by temperature in full scale.

Total exchange volumes were correlated with fractional density difference to develop an exchange model for buoyancy-driven flow during both the steady flow period when the door was fully open, and for the transient flow period when the door was opening and closing. When door swing pumping was negligible, a quasi-steady counterflowing jet model gave a good estimate of flow rate if a time-varying door orifice size was used. The orifice coefficient, which accounts for the effects of viscosity, streamline contraction and mixing between the inward and outward counterflows, varied between 0.6 at large temperature differences and 0.4 at zero temperature difference.

The experimental data were used to determine the nonlinear combination of pumping caused by the swinging motion of the door and the buoyancy-driven counterflow caused by the temperature difference across the doorway. For typical swing speeds it was found that the pumping exchange could be neglected entirely above a temperature difference of 3°C to 5°C. At a temperature difference of zero the volume pumped increased linearly with the speed of the moving door, with a typical exchange volume of about 50% of the swept volume of the door.

INTRODUCTION

Predicting airflow through doorways has important applications in energy conservation, ventilation, smoke control, and pollutant transport. The driving mechanisms are often a combination of density differences, mechanical ventilation, and kinematic effects such as the motion of an occupant through the opening or the motion of the door itself. The present study investigated the combination of two of these mechanisms—buoyancy from density differences and pumping by the swinging door.

Buoyancy-driven flow occurs when there is a difference in density across the opening, and results in counterflow with dense air flowing through the bottom of the opening and less dense air flowing in the opposite direction through the top. In most practical situations the density difference is caused by an indoor-outdoor temperature difference. A static pressure difference across the opening will cause a unidirectional flow from the higher to lower pressure. Typically this pressure arises from mechanical ventilation or wind loading. Finally, exchange flow will occur as an occupant moves through the opening or as the door swings from the closed to open position. In this case, air is drawn behind the person or door surface. These motions also produce vorticity, which promotes transport across the opening. Attention in the past has been focused on the combined effects of buoyancy and static pressure, relevant to large commercial buildings with strong mechanical ventilation and large stack effects (Shaw 1972, 1974).

Before attempting to understand the combined exchange flow produced by buoyancy and door-swing pumping it is necessary to consider each independently. Experimental data from a full-scale test house and a 1:20 scale model are used to determine the limiting conditions where the effects of door-swing pumping are negligible compared to buoyancy-driven flow. The data are also used to establish scaling relationships and to provide the information required in an empirical model of combined pumping and buoyancy-driven flow.

A MODEL OF BUOYANCY DRIVEN FLOW THROUGH DOORWAYS

Steady-State Buoyancy Flow

When there is a difference in fluid density across an exterior or interior opening a buoyancy-driven counterflow will result. Figure 1 illustrates the case of an exterior opening with inside fluid at temperature T_i and density ρ_i, and outside fluid at T_o and ρ_o. An inviscid analysis outlined in Kiel and Wilson (1986) and further developed in Wilson and Kiel (1989) predicts an outflow velocity profile given by

$$U_o' = \left[2g\frac{\Delta\rho}{\rho_o}z\right]^{0.5} \quad (1)$$

The inflow profile is similar, with ρ_o being replaced by ρ_i. Integration across the inflowing and outflowing streams, and application of conservation of volume in a sealed room results in the following expression for inviscid inflow or outflow rate:

$$Q' = \frac{W}{3}\left[gH^3\frac{\Delta\rho}{\rho_e}\right]^{0.5} \quad (2)$$

where

D.E. Kiel is a Ph.D. candidate in the Department of Engineering, University of Cambridge, Cambridge, England. **D.J. Wilson** is Professor, Department of Mechanical Engineering, University of Alberta, Edmonton.

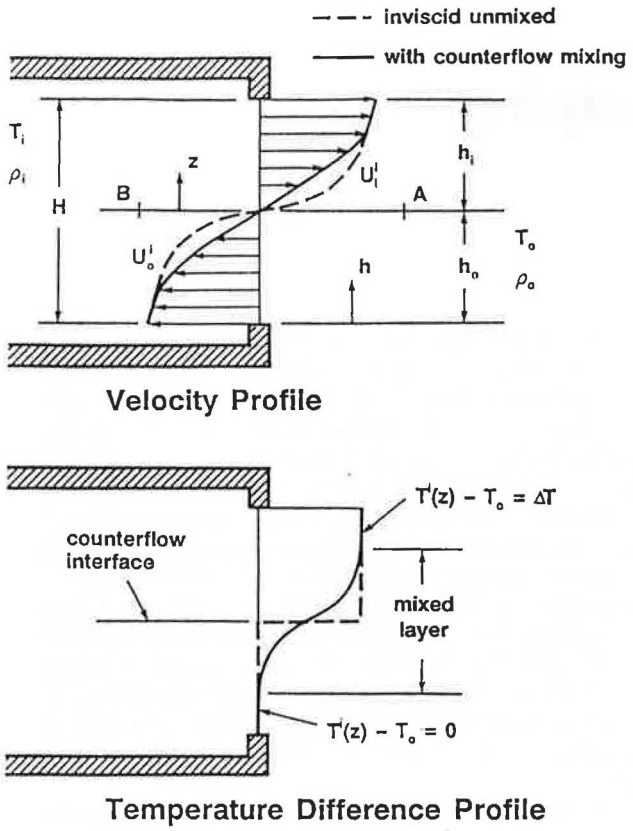

Figure 1 *Inviscid and actual velocity and temperature profiles in the doorway of a sealed room*

$$\rho_e = \rho_i \frac{[1 + (\rho_o/\rho_i)^{1/3}]^3}{8} \tag{3}$$

The effective density ρ_e can be accurately approximated by the average density $\bar{\rho} = (\rho_i + \rho_o)/2$. To account for the effects of viscosity, streamline contraction, and viscous losses, a discharge coefficient C_d is introduced in Equation 2.

$$Q = \frac{C_d W}{3}\left[gH^3\frac{\Delta\rho}{\bar{\rho}}\right]^{0.5} \tag{4}$$

Mixing between the counterflowing streams will occur if the interface is unstable, as illustrated in Figure 2. A volume flux, Q_m, of inflowing air is transported across the interface and returns outdoors, while an equal amount of outflowing air is returned indoors. This transport has a two effects: the net volume flux is reduced by an amount Q_m due to re-entrainment and, in addition, the increased interfacial shear reduces the base flow, Q, as shown by the diminished velocity profile in the mixed layer in Figure 1. Both of these effects are accounted for with a mixing coefficient C_m where

$$Q_n = (1 - C_m)Q \tag{5}$$

In most practical situations it is not possible to measure C_d and C_m separately. For this reason it is convenient to define an overall orifice coefficient K as

$$K = C_d(1 - C_m) \tag{6}$$

such that the net flow rate can be written as

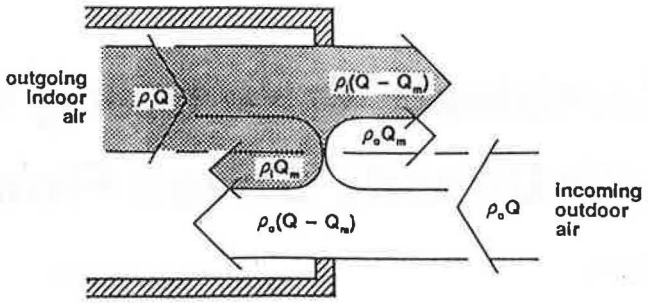

Figure 2 *Reentrainment by cross-stream interfacial mixing between buoyancy-driven counterflowing streams*

$$Q_n = \frac{KW}{3}\left[gH^3\frac{\Delta\rho}{\bar{\rho}}\right]^{0.5} \tag{7}$$

Complete details of the development of these equations are given by Wilson and Kiel (1989).

Buoyancy-Driven Flow During Opening and Closing

Equation 7 applies to an opening of fixed dimensions at a time when steady flow is fully established. In this section we deal with the more realistic case of an opening and closing door. We will begin by assuming that the flow is quasi-steady and account for the time variation of W in Equation 7.

At any time as the door is opening or closing, the minimum opening width is given by $W' = W\cos\theta$, where θ is the angular position of the door. Treating the flow as quasi-steady allows Equation 7 to be written in integral form over the total opening time t_t, which is the sum of the opening time t_o, the fully open hold time t_h, and the closing time t_c.

$$V_n = \int_{t=0}^{t=t_t} \frac{KW'}{3}\left[gH^3\frac{\Delta\rho}{\bar{\rho}}\right]^{0.5} dt \tag{8}$$

Assuming that the orifice coefficient does not vary significantly with door position and that the door swing speed is constant allows Equation 8 to be reduced to

$$V_n = Q_n\left[t_h + \frac{2t_o}{\pi} + \frac{2t_c}{\pi}\right] \tag{9}$$

Other door motions and other types of doors can be dealt with similarly. For example, a sliding door moving at constant velocity would result in a factor of 0.5 rather than $2/\pi$ in Equation 9. The assumption of a constant orifice coefficient is not unreasonable considering that the orifice edge geometry does not vary significantly with door position.

The assumption of quasi-steady flow implies that the flow instantaneously adjusts to the changing opening size while the door is moving. In practice, however, there is a finite amount of time required for the flow to increase to the larger value, so as the door swings open the actual exchange will be less than that predicted by Equation 9. If the door opens slowly and if the density difference is large, the lag time will be small. If, however, the opening velocity is large and the density difference small, the quasi-steady assumption may be invalid. Experimental data will be used to determine the acceptability of the neglecting of acceleration time. If the acceleration time is important we would

expect to see a total exchange less than that predicted by Equation 9, particularly at small density differences.

DOOR PUMPING WITH NO DENSITY DIFFERENCE

The simplest model of door swing pumping is to assume kinematic flow similarity, neglecting viscous forces and fluid inertia. As the door begins to open, air is drawn in behind the door at a velocity proportional to the average speed $\overline{U}_d$ of the door surface (which is equal to the speed of the center of the door)

$$\overline{U}_d = \frac{\pi W}{4t_o} \tag{10}$$

where t_o is the time to swing the door to its fully open 90° position. Because there is no fluid inertia in the kinematic model, the fluid motion stops when the door comes to rest at the fully open position. This is similar to incompressible fluid being drawn behind a piston moving along a cylinder. For kinematic similarity, it is easy to see that the volume V_{po} pumped by the door at $\Delta T = 0$ must be proportional to the volume swept by the moving door V_d

$$V_{po} \propto V_d = \frac{\pi}{4} HW^2 \tag{11}$$

The most important result is that there is no influence of the door velocity $\overline{U}_d$ in models that rely on kinematic similarity.

The kinematic model tends to contradict our intuition. We know from experience that if smoke or odors are being cleared from a room, the pumping rate depends not only on how often a door is swung back and forth, but also on how rapidly the door moves.

In searching for an alternative model we must keep in mind that the room into which the door opens is sealed, requiring the volume flow rate of outdoor air in through the doorway to be balanced by an equal outflow of indoor air. A simple dynamic model for pumping can be formulated by providing the inflow air with an impulsive velocity equal to the door velocity, and then allowing the flow rate to decrease as turbulent shear between the inflowing and outflowing streams decelerates the flow. The parameter in this analysis is the turbulent eddy viscosity ν_T in the counterflowing shear layer. We assumed the general form $\nu_T \propto U\delta(\nu/U\delta)^a$, where U is the instantaneous inflow velocity, δ is the shear layer thickness, and ν is the molecular kinematic viscosity. The exponent a is experimentally determined, and varies from $a = 0$ for fully turbulent flow with no Reynolds number dependence to $a = 1.0$ for laminar flow where $\nu_T = \nu$. Equating the counterflow shear forces to the flow deceleration and integrating twice leads (after considerable manipulation) to

$$V_{po} \propto V_d \left[\frac{\overline{U}_d \delta}{\nu}\right]^a \tag{12}$$

Using Equation 11, this becomes

$$V_{po} \propto HW^2 \left[\frac{\overline{U}_d \delta}{\nu}\right]^a \tag{13}$$

laminar flow, $a = 1.0$ and

$$V_{po} \propto \frac{HW^2 \overline{U}_d \delta}{\nu} \tag{14}$$

and for fully developed turbulent flow $a = 0$ and

$$V_{po} \propto HW^2 \tag{15}$$

These are surprising results, because they show that a fully turbulent impulsive flow model predicts no effect of door velocity $\overline{U}_d$. Measurements in a full-scale house with air and in a model with water allowed both viscosity and door swing speed to be varied in order to test these kinematic and impulse flow models.

COMBINED BUOYANCY AND PUMPING FLOW

In most practical problems both pumping exchange and buoyancy-driven exchange will occur. We cannot expect simple addition of the two flows to provide an estimate of their combined effect because each mechanism tends to interfere with the other's ability to promote exchange. Vorticity is produced at the edge of the opening door and in the region of flow between the inbound and outbound flow. This vorticity will tend to roll up into a standing vortex, further decoupling the door from the outside air and from the size and shape of the inside room. The counterflowing currents will sweep vorticity away, reducing its ability to promote exchange as well as carrying away entrained fluid from behind the door. Similarly the vorticity produced by the moving door will tend to disrupt the coherent structure of the counterflow. The degree to which the two mechanisms influence one another depends upon their relative strength. For a given door velocity buoyancy forces will dominate at large temperature differences and the flow will be that predicted by buoyancy alone. At a small temperature difference door swing pumping will dominate. Between these two extremes the exchange flow that results depends on the combined effect of the two mechanisms.

These ideas are illustrated in Figure 3. The *predicted buoyancy* line is the exchange that would result from buoyancy alone, as given by Equation 9. Below some critical value of fractional density difference, the effects of pumping start to be important and we see a departure from the predicted buoyancy curve. As the density difference approaches zero, the total exchange approaches an intercept of V_{po}, which is the volume exchanged by pumping alone. The curve labeled *actual buoyancy* is shown to emphasize

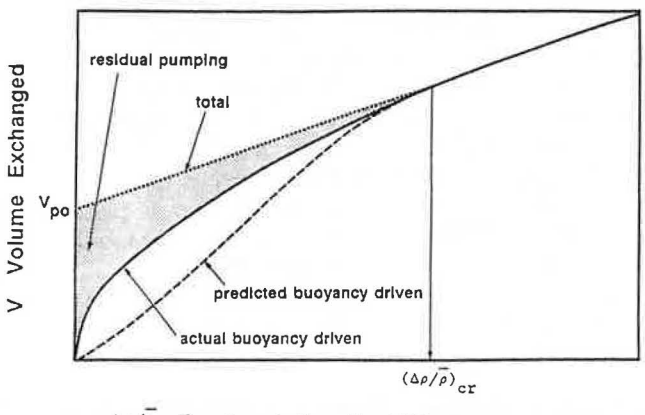

Figure 3 *Idealized volume exchange curves for combined buoyancy-driven flow and pumping flow during a typical door opening/closing cycle*

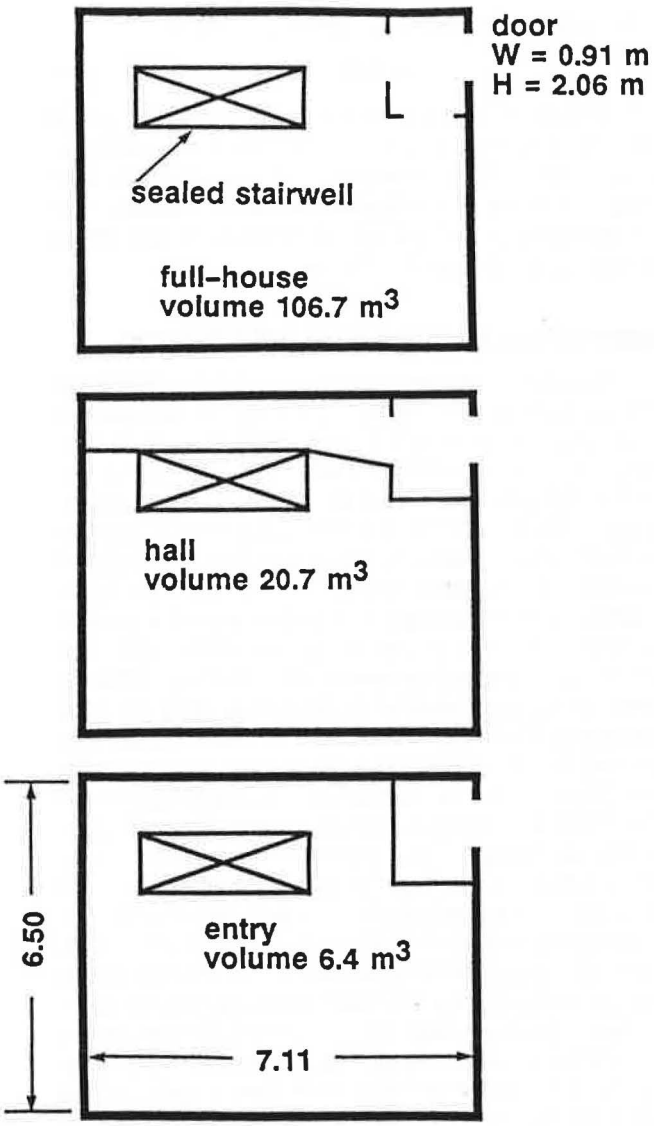

Figure 4 *Interior partition layouts used in full-scale and model experiments*

that the buoyancy-driven flow is modified by the swinging action of the door. The actual pumped contribution is the difference between the total exchanged and the actual buoyancy exchange. From a practical point of view it is impossible to distinguish between the pumping contribution and the actual buoyancy contribution. For this reason it proves most useful to identify a volume called the *residual pumped volume*, V_p, which is defined as the volume exchanged in excess of that predicted by buoyancy alone.

The concept of residual volume (rather than a volume flow rate) is attractive if the pumped volume does not depend on how long the door is fully open because it can then be thought of as a *per opening quantity*.

The total exchange would then be the sum of the buoyancy flow, given by Equation 9, and the residual pumped volume, V_{po}.

Departure from Buoyancy Prediction Due to Pumping

As illustrated in Figure 3, the actual exchange flow departs from the buoyancy prediction at a critical value of fractional density difference. The value depends on the relative strength of inertial forces caused by the door motion relative to the buoyancy forces produced by the density difference. The buoyancy forces are dependent on the density difference and the door height, while the inertial forces depend on the velocity of the door. The ability of the pumping flow to disrupt the buoyancy flow may also depend on the contact surface between the flows. For example the buoyancy flow through a tall narrow door may be less disrupted by pumping than it would if the door was short and wide. From this we conclude that

$$\left[\frac{\Delta\rho}{\bar{\rho}}\right]_{cr} = fcn(\bar{U}_d, H, H/W) \qquad (16)$$

Dimensional analysis suggests that a Froude number criterion should apply. This indicates that the critical fractional density difference shown in Figure 3 should scale with $\bar{U}_d^2$. Experimental data will be examined to determine the appropriate relationship.

MEASURING EXCHANGE FLOWS

Description of Full-Scale Facility

Full-scale measurements of air exchange through an exterior doorway were carried out at the Alberta Home Heating Research Facility. The test house used in these studies was a single-story building with overall floor dimensions of 6.5m × 7.1m, an interior wall height of 2.4m, and no interior walls. A single exterior door 2.06m high and 0.91m wide was opened and closed by a remotely controlled actuator, providing accurate and repeatable times for opening, closing, and fully open. From Equation 11 the swept volume of the door during a 90° swing is V_d = 1.28m³. The effect of interior walls and room size was investigated using partitions to create three different interior volumes, as shown in Figure 4.

The air exchange was measured using sulfur hexaflouride as a tracer gas. A quantity of gas was injected, thoroughly mixed with the interior air, and the concentration measured using an infrared gas analyzer. Following the exchange, the interior air was again thoroughly mixed and the final concentration determined. Using the initial concentration, final concentration, and the interior volume, the total exchange was determined.

Thermocouple arrays were used to determine spacial information about the air flow patterns inside the house, such as temperature profiles and gravity current front motion. More information about the experimental facility may be found in Wilson and Kiel (1989).

Description of 1:20 Scale Model

A 1/20th plexiglass scale model was constructed and suspended in a fresh water reservoir from a load cell, as shown in Figure 5. The model was filled with saline solution, the density of which was selected to match the full-scale indoor-outdoor density difference to be simulated. The model door was then opened and closed by a computer-controlled stepping motor. As the dense solution poured from the top of the inverted door during the opening-closing cycle there was an inflow of lighter fresh water from the reservoir to replace it. The changing weight of the model as sensed by the load cell was continuously monitored.

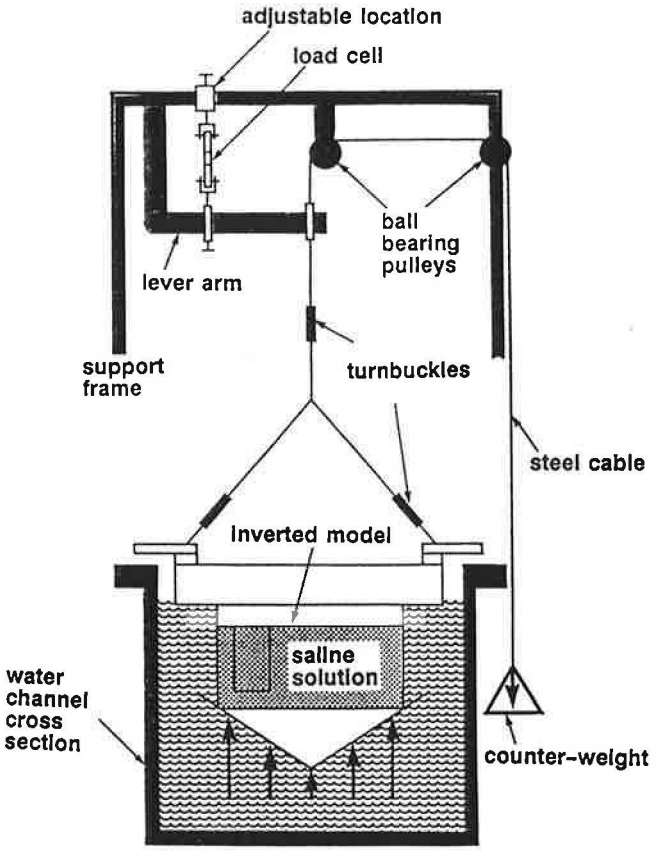

Figure 5 *Differential weight measurement system used in the 1:20 scale model to determine exchange volumes*

At small density differences, the weight change was very small and the differential weight measurement system was prone to error. Electrical conductivity probes were used instead to determine the net volume exchange in a manner analogous to the tracer gas technique in full scale. To simulate temperature differences very near zero, alcohol-saline solutions were used to produce neutral buoyancy solutions which still had sufficient salt present to provide accurate exchange measurements. Multiple probes were also used to measure point concentrations within the flow, analogous to local temperature measurements in the full-scale flow. This provided information on the frontal position of the intruding gravity current and a measure of interfacial mixing across the counterflow boundary.

SCALE MODELING CRITERIA

There are several advantages associated with scale-model simulations to gain insight into full-scale flow problems. Model studies usually can be accomplished in a shorter time, provide complete control over experimental parameters, allow for the use of alternative measurement techniques, and permit modifications to be made easily and inexpensively. One difficulty with scale modeling is the invariable mismatch in dynamic similarity between the model and full-scale flows. It is essential to carefully consider the relevant scaling relationships to ensure that the associated difficulties are minimized and clearly understood.

In this study Froude number similarity was used throughout and, with some minor exceptions, provided satisfactory results. Stated in terms of forces, Froude number similarity requires that the ratio of inertia forces to buoyancy forces be identical at all geometrically similar points in the model and full-scale flow, where the Froude number is defined as:

$$Fr = \left[\frac{L}{g't^2}\right]^{0.5} \tag{17}$$

where g' is the effective gravitational acceleration defined as $g(\Delta\rho/\bar{\rho})$. The Froude number is usually written in terms of velocity, $F_r = (U^2/g'L)^{0.5}$. Here we use t, the velocity time scale in $U = L/t$, to express the Froude number in terms of the fundamental variables of length and time.

Equating the model and full-scale Froude numbers,

$$\left[\frac{L_M}{g'_M t_M^2}\right]^{0.5} = \left[\frac{L_F}{g'_F t_F^2}\right]^{0.5} \tag{18}$$

defining length, time, and effective gravity scale factors L_S, t_S, and g'_S,

$$L_S = \frac{L_F}{L_M} \tag{19}$$

$$t_S = \frac{t_F}{t_M} \tag{20}$$

$$g'_S = \frac{g'_F}{g'_M} \tag{21}$$

and combining Equations 18, 19, 20, and 21 results in the following conditions for Froude number similarity:

$$\frac{L_S}{t_S^2 g'_S} = 1 \tag{22}$$

The model was 1/20 the size of the test house and thus $L_M = 20$, and the fractional density difference in the model was identically matched to the full scale so $g'_S = 1$. Substituting these scales into Equation 22 results in a Froude number buoyancy time scale of $\sqrt{20}$. This buoyancy time scale implies that events occur 4.47 times faster in the model compared to full scale. For example, to simulate an opening time of 3s in full scale requires the model door to be opened in 3/4.47s.

To allow easy comparison of model and full-scale results, the model data presented in the figures and tables have been converted to equivalent full-scale values using the 20:1 length scale and 4.47:1 time scale. For example, the exchanged volumes in the model were multiplied by 20^3, and the opening times by 4.47 to give their full-scale equivalents. It should be kept in mind that these conversions require that both the pumped and density-driven flows be dominated by buoyancy and inertia forces, and thus are insensitive to viscous forces.

The decision to match Froude numbers means that other potentially relevant nondimensional parameters were not matched. There is no difficulty with this as long as the flow regime is dominated by buoyancy and inertial forces. If, however, at small density differences viscosity becomes more important than buoyancy, then the Reynolds number may be the more relevant parameter and errors in the predictions will result. If the flow of interest spans more than one flow regime, it may not be possible to accurately model both using a single time scale.

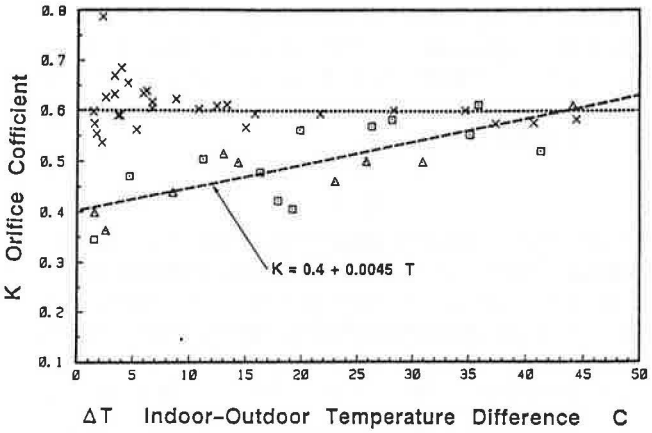

Figure 6 *Comparison of model and full-scale doorway orifice coefficient variation with indoor-outdoor temperature difference under steady-flow conditions (× 1:20 scale model; full scale; □ full house; △ hall*

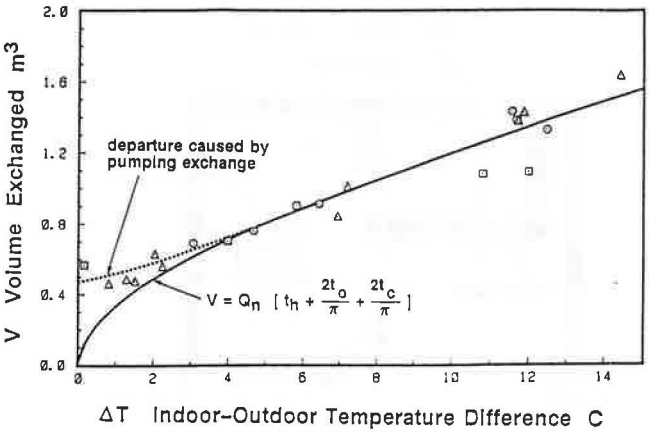

Figure 7 *Full-scale volume exchange measured during short duration opening/closing cycles for different interior layouts (□ full-house, △ hall, ○ entry; T_i = 22°C; t_o = t_c = 3.7 s; t_h = 0.5 s; U_d = 0/19 m/s)*

Following the same procedure for Reynolds number as was applied to the above Froude number results in the following scale relationship:

$$\frac{L_S^2}{t_S \nu_S} = 1 \qquad (23)$$

where ν_S, the viscosity scale, is equal to 12.7 for the water and air combination used in this study. Substituting the length scale and viscosity scale in Equation 23 gives a time scale of 31. Clearly it is not possible to satisfy both the Froude number time scale of 4.47 and the Reynolds number time scale of 31 at the same time. Choosing to match the Froude number results in mismatch in Reynolds number by a factor of seven because the difference in viscosity between the water model and the full-scale air system helps to compensate for the 20:1 length scale difference.

$$Re_F = 7Re_M \qquad (24)$$

We can calculate the full-scale Reynolds number for pumping flow using the door width as the characteristic length and the average door surface velocity as the characteristic velocity. The full-scale Reynolds number was 14,000 and the model Reynolds varied between 2000 and 4000, depending on the door velocity. These are probably sufficiently high for the flow to be inertially dominated and therefore viscous effects may be negligible.

If there is a transition in the flow regime from buoyancy-dominated to viscous-dominated flow, we will see a divergence between the model and full-scale results due to time scale mismatching. Experimental data will be examined with these ideas in mind.

EXPERIMENTAL RESULTS

Steady-State Buoyancy-Driven Flow

A series of exchange experiments were conducted in which the fully open hold time was gradually increased. Correlating the volume exchange with fully open time allowed the net steady flow rate, Q_n, to be determined. The fully open duration was long compared to the opening and closing time to ensure that a true measure of steady flow was made. Using these flow rates in Equation 7 allowed the value of overall orifice coefficient to be determined and values of K are plotted in Figure 6 for both the model and full-scale test house.

From Figure 6 we see that the model orifice coefficient is constant at 0.6, while the full-scale coefficient decreases from 0.6 at large temperature differences to about 0.4 at a temperature difference of zero, as described by

$$K = 0.4 + 0.0075\Delta T \qquad (25)$$

The variation in full-scale orifice coefficient is in close agreement with data obtained by Fritzsche and Lilienblum (1968) for flows through cold room doors. Wilson and Kiel (1989) examined the data closely to determine the cause of the observed differences between the model and full-scale results. Measured temperature and concentration profiles showed that the increased net flow rate in the model (which produces the higher orifice coefficient) is caused by the absence of interfacial mixing between the counterflowing streams. This is one of the effects of Reynolds number mismatch.

It must be remembered that the model flow rates are converted to full-scale units using the length scale of 20 and a time scale of 4.47 based on Froude number similarity. Froude number similarity does a good job of matching the results at large density differences where the secondary effect of interfacial mixing does not influence the net flow rate. It was also found that Froude number similarity resulted in excellent agreement between model and full-scale data for other buoyancy-dominated aspects of the flow such as gravity current frontal velocity. From this we may conclude that the buoyancy flow is well modeled in a gross sense, but that some details of the counterflow mixing process are inaccurately modeled, but can be corrected for using a modified orifice coefficient.

Short Duration Exchange

Having now examined the problem of steady flow we turn out attention to exchange during the opeing and closing period. Figure 7 shows the total exchange that occurs when the door was fully opened for a short period of time such that the exchange was dominated by flow during the

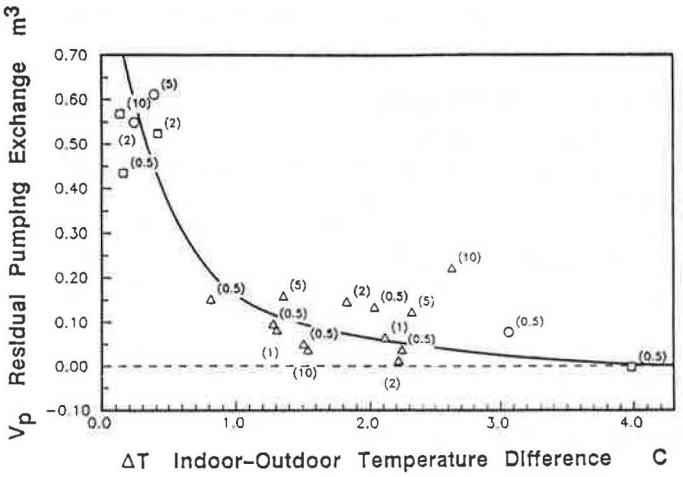

Figure 8 *Full-scale measurements of the effect of fully open hold time on residual pumping (□ full-house, △ hall, ○ entry; t_h = ( )s; t_o = t_c = 3.7 s; U_d = 0.10 m/s)*

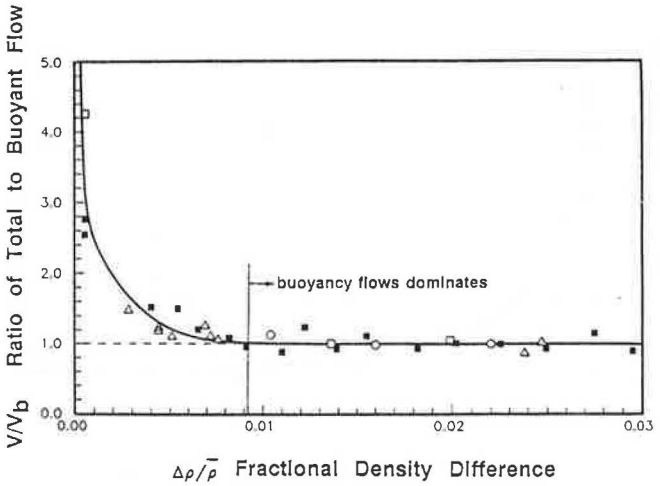

Figure 9 *Ratio of total volume exchange to predicted buoyancy exchange at a low door velocity measured in the 1:20 scale model and full scale (Full scale: □ full-house, △ hall, ○ entry; T_o = t_c = 3.7 s; t_h = 1.0 and 0/5 s; U_d = 0.19 m/s. Model: ■ full-house; t_o = t_c = 3.6 s; t_h = 1.0 s; U_d = 0.20 m/s)*

opening and closing periods. Equation 9, which is based on a quasi-steady flow assumption, is used to predict the buoyancy-driven exchange. The value of K used in this prediction is given by Equation 25, which accounts for counterflow interfacial mixing effects that are a function of density difference.

The quasi-steady approximation of Equations 9 and 25 gives good estimates of the total volume exchanged for temperature differences greater than about 4°C. Below 4°C the exchange diverges from that predicted by quasi-steady buoyancy flow and approaches a value of approximately 0.5m³ at $\Delta T = 0$. This exchange is about 40% of the swept volume of the door, for the particular swing speed of $\bar{U}_d$ = 0.2m/s used in all the tests. Agreement is also good at temperature differences larger than those shown on Figure 7, but only the lower range has been shown to clearly illustrate the departure region. Below 4°C the door swing motion begins to influence the total exchange. In this range, between 0°C < ΔT < 4°C, buoyancy and pumping combine to produce an exchange which is greater than that predicted by buoyancy alone.

At small density differences we expected to see the effects of buoyancy flow acceleration time. As discussed previously this would tend to reduce the exchange below that predicted by Equation 9. Clearly no such departure is apparent in Figure 7 above 4°C.his does not mean that the effect is not present, but it may only become important at density differences smaller than those at which pumping exchange begins to cause increased flow, thereby obscuring the delayed flow effect of buoyancy acceleration time.

Effect of Hold Time on Residual Pumping

Another critical question is whether the flow induced by the motion of the door persists after the door is fully open. Figure 8 shows the residual pumping exchange that occurs for fully open hold times between 0.5s and 10s. If the flow persisted after the door was fully open, we would expect to see larger values of residual pumping exchange associated with longer hold times. From Figure 8 it is apparent that this is not the case. It is possible that at door velocities greater than those tested here the flow will persist for a longer time. Based on these data we conclude that for door velocities of approximately 0.2m/s and slower, it is acceptable to consider the residual volume exchanged as independent of the fully open hold time, and is therefore a *per opening* quantity.

From Figures 7 and 8 there appears to be no significant variation in exchange with room size or layout. This is not the case if very long hold times are used because the flow will start to diminish once the gravity current has struck the interior wall and reflects back to the door. The data examined here is for sufficiently short hold times that the buoyancy flow has not yet begun to decrease. The residual pumped volume concept and values still apply even if the buoyancy exchange starts to decrease (due to the room being of finite size) because the pumping exchange occurs early in the exchange process. In this case the buoyancy prediction given by Equation 9 will be in error and a model of diminishing flow must be used (Kiel and Wilson 1986).

Critical Fractional Density Difference

The departure from buoyancy-dominated exchange is evident in both Figures 7 and 8. This departure point can be more accurately established by considering the ratio of the total volume exchanged to that predicted by buoyancy alone, V/V_b, as shown in Figure 9. This clearly shows that above a fractional density difference of 0.009, buoyancy flow alone is important. The agreement between the model and full-scale data is very good and strongly suggests that the departure is dependent on inertial effects and not on viscous effects. This is because Froude number scaling has been used to set the model time scaling as $\sqrt{L_s}$ and is independent of viscosity.

The fractional density difference at which departure from buoyancy-dominated flow occurs will depend on the inertial forces associated with the door motion and thus on the door velocity. To evaluate this, four different swing speeds were tested in the model. The good agreement between the model and full-scale data in Figure 9 suggests that the model results should provide an accurate predic-

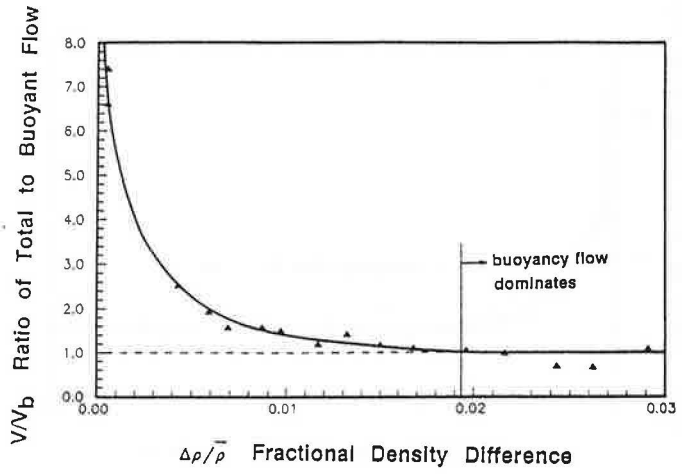

Figure 10 *Ratio of total volume exchange to predicted buoyancy exchange for a high door velocity measured in the 1:20 scale model with full-house layout ($t_o = t_c = 1.9$ s; $t_h = 1.0$ s; $U_d = 0.37$ m/s)*

tion of the full-scale departure values using the time scale of $\sqrt{L_s}$ based on Froude number similarity.

Figure 10 shows model data plotted in a similar format to Figure 9, for a door velocity of 0.37m/s, compared to 0.20m/s in Figure 9. The departure point has clearly shifted to approximately 0.019 from 0.009 in Figure 8. The departure points were determined similarly for the two other swing speeds tested.

TABLE 1
Critical Fractional Density Difference for Suppression of Door Swing Pumping Effects

	Door Velocity, $\bar{U}_d$, m/s	Critical Density Difference $\Delta\rho/\bar{\rho}$
Model*	0.37	0.019
	0.29	0.012
	0.23	0.012
	0.20	0.009
Full Scale	0.19	0.009

*model data scaled up

From these results it was found that the critical fractional density difference (Table 1) is directly proportional to the door velocity

$$\left[\frac{\Delta\rho}{\bar{\rho}}\right]_{cr} = 0.046\bar{U}_d \qquad (26)$$

This linear dependence of critical density difference on swing speed is unexpected and puzzling. What we expected was a critical Froude number based on door swing speed. Because it is the door height, H, that controls the average velocity of the counterflowing streams, it is reasonable to define a door swing Froude number by

$$Fr_d = \left[\frac{\bar{U}_d^2}{g\left(\frac{\Delta\rho}{\bar{\rho}}\right)H}\right]^{0.5} \qquad (27)$$

If a critical value of Fr_d occurred at the point where door swing effects are suppressed by density difference effects, we would expect $(\Delta\rho/\bar{\rho})_{cr} \propto \bar{U}_d^2$. Instead we found the linear dependence in Equation 26.

Nondimensional Groupings

It is always attractive to formulate nondimensional groupings to allow interdependent variables to be quantified through single parameters. To form appropriate nondimensional groupings requires the selection of appropriate length and time scales and in some cases there is ambiguity as to the correct length scales to be used. Only one door size was tested in the experimental study presented here and for this reason, data will be presented in terms of the measured variables, such as volume exchanged or density difference, rather than normalized parameters. Although this may not be as attractive, it is at least honest, and prevents the construction of nondimensional groupings that may not apply for door sizes and density differences that are significantly different than those tested here.

Pumping Exchange at Zero Temperature Difference

Having established the point of departure from buoyancy-dominated flow we now turn our attention toward the opposite extreme of zero density difference and consider the effect of door velocity on the volume pumped. For the same four swing speeds discussed above the following volumes were measured at $\Delta\rho/\bar{\rho} = 0$. (see Table 2).

TABLE 2
Door Swing Pumping at Zero Temperature Difference

	Door Velocity, $\bar{U}_d$, m/s	Volume Exchanged, V_{po}, m³
Model*	0.37	0.72
	0.29	0.61
	0.23	0.52
	0.20	0.43
Full Scale	0.19	0.50

*model data scaled up

On the basis of these results it is apparent that at a density difference of zero, the pumped volume is proportional to the door velocity as given by

$$V_{po} = 2.3\bar{U}_d \qquad (28)$$

and is independent of the fluid kinematic viscosity, ν.

Two models of pumping flow were proposed—a kinematic flow model and an impulsive flow model. The kinematic model, which predicted no dependence on door velocity, is clearly incorrect. The model experiments support the linear dependence of pumped volume, V_{po}, on door swing speed, $\bar{U}_d$, given by the laminar shear flow ($a = 1.0$) deceleration theory in Equation 14. However, comparing V_{po} for the water model and the air full scale in Table 1, we see that there is no dependence on fluid viscosity even though the water in the model had a kinematic viscosity 12.7 times less than air. But, if there is no dependence on viscosity there should also be no effect of door swing speed (which is what is predicted by the fully turbulent $a = 0$ shear deceleration model in Equation 15). All we can conclude at this stage is that the impulsively started,

shear-decelerated flow model does not give realistic predictions.

The good agreement obtained between full-scale and model data at a density difference of zero, using Froude number time scaling, suggests that the pumping process is totally inviscid. If it were not, Reynolds number scaling would have applied, requiring a time scale of 31, not 4.47. This would have resulted in considerable mismatch between the model and full-scale results. We must conclude from this that the pumping time scale is similar to, or the same as, Froude number time scaling.

Normalizing Residual Pumping Exchange

Having examined the asymptotic extremes of pumping exchange we will now consider the intermediate regime of combined pumping and buoyancy-driven flow. From Equation 26 we have concluded that the critical fractional density difference can be normalized with door velocity using the ratio $(\Delta\rho/\bar{\rho})/\bar{U}_d$ and the data will collapse to a value of approximately 0.046s/m. At the opposite extreme of zero density difference, it was shown that the pumped volume can also be normalized with the door velocity as $V_{po}/\bar{U}_d$ with the data collapsing to a value of approximately 2.3m²s. With these relationships in mind, data from all four door velocities are combined in Figure 11.

As expected, the data collapses nicely at a density difference of zero and at the critical departure point. The data for each door velocity appear to follow a similar functional form between the two asymptotic extremes. Scatter in all the data is not much greater than the scatter within any individual set of data, so it is reasonable to approximate all four velocities with the same empirical function. The function

$$\frac{V_p}{\bar{U}_d} = \frac{2.3}{1 + \left[45\frac{\Delta\rho/\bar{\rho}}{\bar{U}_d}\right]^4} \qquad (29)$$

was chosen because it becomes diminishingly small above the critical departure point and is simple in form.

These results may now be combined to construct a model of combined buoyancy and pumping flow. This model is simply the sum of buoyancy-driven flow and residual pumping flow, $V = V_p + V_b$, which is the combination of Equations 7, 9, and 29.

$$V = \frac{KW}{3}\left[gH^3\frac{\Delta\rho}{\rho}\right]^{0.5}\left[t_h + \frac{2t_o}{\pi} + \frac{2t_c}{\pi}\right] + \frac{2.3\bar{U}_d}{1 + \left[45\frac{\Delta\rho/\rho}{\bar{U}_d}\right]^4} \qquad (30)$$

This equation is valid only for doors of about the same size as the door tested here because the residual pumping contribution is not properly nondimensionalized for the door size.

EFFECT OF OCCUPANT MOTION ON EXCHANGE

Up to this point the effects of occupants moving through the opening has been neglected. Two different and quite opposite effects can be imagined. The motion of

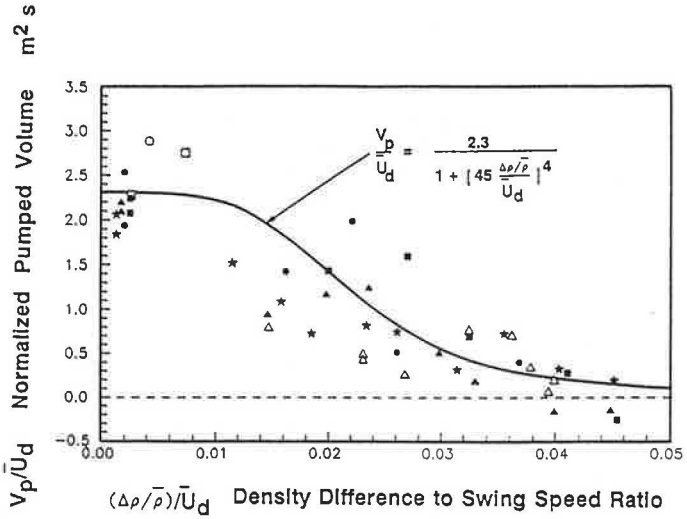

Figure 11 *Normalization of residual pumping exchange using door velocity (Full scale: □ full-house, △ hall, ○ entry; U_d = 0.19 m/s; t_h = 0.5, 1.0, and 2.0 s. Model: full-house; ▲ U_d = 0.37 m/s; ★ U_d = 0.29 m/s; ● U_d = 0.24 m/s; ■ U_d = 0.20 m/s; t_h = 1.0 s)*

the occupant may increase exchange by entraining outside air in his or her wake in a manner similar to the door itself, or decrease the exchange by constricting the opening size and disrupting the buoyancy counterflow.

Shaw (1976) studied occupant entrainment transfer through an open sliding door 0.90m wide and 2.05m high, at a temperature difference of zero. He determined that exchange volumes ranged from 0.29m³ for a fast walk to 0.087m³ for a slow walk. The importance of occupant-entrained air will diminish with larger temperature differences in the same way residual pumping exchange diminishes.

CONCLUSIONS

- The assumption of quasi-steady buoyancy-driven flow during door opening and closing gives an accurate estimate of buoyancy-driven exchange flow. The initial acceleration time of the buoyancy current was compensated for by the door swing pumping and can therefore be neglected.
- Modeling buoyancy-driven flow is best achieved using Froude number similarity; however, corrections to the orifice coefficient are required to account for differences in interfacial mixing of the counterflowing streams.
- At a density difference of zero the model was found to predict the same pumped volume measured in full scale by using a time scale equal to the square root of length scale, which is the buoyancy time scale.
- At a density difference of zero the total exchange volume was found to be proportional to the door swing speed and independent of fluid viscosity.
- Above a critical ratio of density difference $\Delta\rho/\bar{\rho}$ to door swing speed $\bar{U}_d$, density-driven flow suppressed all effects of door swing pumping. This critical ratio was the same in model and full scale

when Froude number time scaling was used on the swing speed.

- Between zero density difference and the critical fractional density difference departure point, data from a range of door velocities were found to follow a similar functional form if the residual exchange volume and the fractional density difference were normalized with the door velocity. An empirical relationship was developed to estimate the residual volume.

Further experimental investigation of the scaling relationships is required before nondimensional parameters can be formulated with certainty. For this reason the empirical relationship developed in this report should be used with caution if the door is substantially different in size from the door tested here.

ACKNOWLEDGMENTS

This study was supported by research grants from Energy Mines and Resources Canada and the Natural Sciences and Engineering Research Council of Canada. Assistance from a Canada Mortgage and Housing Corporation scholarship and an ASHRAE grant-in-aid to D.E. Kiel are gratefully acknowledged.

NOMENCLATURE

C_d = discharge coefficient
C_m = mixing coefficient
F_r = Froude number, Equation 27
g = gravitational acceleration, ms^{-2}
g' = effective gravitational acceleration, ms^{-2}
h = layer thickness
H = opening height, m
K = orifice coefficient
L = length
Q = flow rate, m^3s^{-1}
Re = Reynolds number
t = time, s
V = volume, m^3
W = doorway opening width, m
W' = instantaneous opening width, m
z = height above counterflow interfacial streamline

Greek symbols

δ = shear layer thickness
Δ = indoor-outdoor difference
θ = door angle, °
η = dynamic viscosity, $kg,m^{-1}s^{-1}$
ν = kinematic viscosity, m^2s^{-1}
ρ = density, $kg\ m^{-3}$

Subscripts

c = closing
d = of the door
F = full scale
h = hold
i = indoor
m = interfacial mixing
M = model
n = net
o = outdoor or opening
p = pumped
po = pumped at zero temperature difference
S = scaling factor
t = total
T = turbulence

Superscripts

i = inviscid

REFERENCES

Brown, W.G.; Wilson, A.G.; and Solvason, K.R. 1963. "Heat and moisture flow through openings by convection." *ASHRAE Journal*, September, pp. 49-53.

Brown, W.G., and Solvason, K.R. 1961. "Natural convection through rectangular openings in partitions—1." *Int. J. Heat and Mass Transfer*, Vol. 5, pp. 859-868.

Fritzsche, C., and Lilienblum, W. 1968. "New measurements for the determination of the cold losses at the doors of cold rooms" (in German). *Kaltetechnik—Klimatisierung*, 20, Jahrgang Heft 9.

Kiel, D.E., and Wilson, D.W. 1986. "Density driven flows through open doors." *Proceedings of the Seventh Air Infiltration Center Conference*, Stratford-Upon Avon, September.

Shaw, B.H. 1972. "Heat and mass transfer by natural convection and combined natural convection and forced air flow through large openings in a vertical partition." Institute of Mechanical Engineers Conference, Vol. CS19.

Shaw, B.H. 1976. "Heat and mass transfer by convection through large rectangular openings in a vertical partitions." Ph.D. Thesis, Department of Mechanical Engineering, University of Glasgow.

Shaw, B.H., and Whyte, W. 1974. "Air movement through doorways; the influence of temperature and its control by forced airflow." *Building Services Engineer*, Dec., Vol. 42.

Wilson, D.J., and Kiel, D.E. 1989. "Density driven counterflow through an open door in a sealed room." Submitted to *Building and Environment*.